Two-neutrino double-beta decay of ^{82}Se to ^{82}Kr

Author: Beatriz Benavente de Lucas
Facultat de Física, Universitat de Barcelona, Diagonal 645, 08028 Barcelona, Spain

Advisor: Javier Menéndez Sánchez

Abstract: In this study, we investigate the two-neutrino double-beta decay ($2\nu\beta\beta$) of ^{82}Se to the first excited 0_2^+ state of ^{82}Kr within the framework of the nuclear shell model. We consider four different interactions and we analyze the validity of these interactions in reproducing the experimental properties of the initial and final states of the decay. The calculated half-life for the decay is determined using as reference the comparison between the calculated decay of ^{82}Se to the ground state of ^{82}Kr and experimental data. We find an interval for the predicted half-life for this transition that is $T^{2\nu}_{1/2}(^{82}\mathrm{Se}, 0^+_{gs} \to 0^+_2) = (3.5 - 170) \cdot 10^{22}$ yr.

I. INTRODUCTION

The Standard Model of particle physics (SM) is a widely accepted theoretical framework that describes three of the fundamental forces governing the universe. Nevertheless, unresolved questions persist within this theoretical framework, as for instance why there is a predominance of matter over antimatter in the observable universe. Extensions of the SM allow some transitions forbidden in this model. An example is the neutrinoless double-beta decay, $0\nu\beta\beta$ decay, a special decay of an atomic nucleus.

In double-beta decay, two neutrons convert into two protons, accompanied by the emission of two electrons. According to the SM, this decay, called two-neutrino double-β decay ($2\nu\beta\beta$ decay), involves the emission of two antineutrinos, maintaining an equilibrium between matter and antimatter and preserving the principle of conserving lepton number. In contrast, in the neutrinoless decay no antineutrinos are emitted. This reaction, which has yet to be observed, challenges the SM, violating lepton-number conservation, creating matter ($2e^-$) but no antimatter ($0\overline{\nu}$) [1]. This specific decay is the focus of on-going experimental searches. The empirical observation of such reactions would signify the confirmation of physics beyond the SM.

The exploration of $0\nu\beta\beta$ decay serves as a driving force behind our investigation into the $2\nu\beta\beta$ decay. The initial and final nuclear states are common in both scenarios. Therefore, the methodologies applied in the investigation of $2\nu\beta\beta$-decay matrix elements are also applicable to the neutrinoless case. Testing and refinement of the matrix elements for the two-neutrino scenario, $M^{2\nu}$, have the potential to improve the accuracy in the determination of the matrix elements for the neutrinoless case, $M^{0\nu}$. This is important because there is no experimental data for the $0\nu\beta\beta$ decay, so the values of the matrix elements governing this decay must be derived from theoretical calculations. One remarkable aspect of this investigation is the extremely long half-lives associated with $2\nu\beta\beta$ decay. Some nuclei showing this decay are ^{130}Te and ^{136}Xe, exhibiting half-lives on the order of $10^{20} - 10^{21}$ years. This prolonged timescale presents a challenge for experimental projects aiming to observe these rare decay events. Thus, reducing the uncertainty assists significantly the experimental search for this reaction.

We specifically direct our attention to the decay of ^{82}Se into ^{82}Kr. With this motivation in mind, our objective is to predict the half-life of the $2\nu\beta\beta$ decay to the first 0_2^+ excited state of ^{82}Kr. The study of the decay to the ground state will serve a reference, given that it is well-established experimentally [2].

One of the many challenges in nuclear physics is to describe the interactions within nuclei. Our approach centers on the nuclear shell model. To tackle this challenge, we employ shell-model interactions derived in previous studies. In order to achieve the goal of this work, we firstly study the spectrum of both ^{82}Se and ^{82}Kr to assess the ability of the different interactions to reproduce the nuclear structure of these nuclei. Subsequently, we calculate the matrix elements for the $2\nu\beta\beta$ decay to the ground state, $M^{2\nu}(0^+_{gs})$, enabling the computation of half-life predictions. Typically, theoretical calculations predict shorter half-lives than those observed experimentally [3]. Due to this fact a correction is made by a 'quenching' factor.

Similarly, we calculate the matrix elements for the decay to the first excited state, $M^{2\nu}(0^+_2)$. Finally, we estimate the half-life for the $2\nu\beta\beta$ decay to the first 0_2^+ excited state of ^{82}Kr. This result has not been experimentally measured; nevertheless, there is experimental interest [4].

II. NUCLEAR SHELL MODEL

In order to study the complex system which is an atomic nucleus we need to solve the non-relativistic many-body Schrödinger equation:

$$H\,|\psi\rangle = E\,|\psi\rangle\,, \tag{1}$$

where H is the Hamiltonian describing the system, $|\psi\rangle$ is the wave function describing the state of the system and E the energy of the system.

The complexity of nuclear systems renders it impossible to accurately describe them analytically. This is the

reason we use models to understand the nuclear structure. The nuclear shell model, developed by Mayer and Jensen, is a many-body method for solving the nuclear problem with an effective many-body Hamiltonian [5].

The Hamiltonian consists of distinct components: one involving one-body operators, H_0, and another involving two-body operators, W:

$$H = H_0 + W. \tag{2}$$

Assuming the nuclear mean field model, we can approximate nucleons as independent particles under the same nuclear potential. This constitutes the one-body Hamiltonian, H_0. The one-body part includes, to begin with, the kinetic energy of the independent nucleons, $T(r_i)$ and a potential central term, $V(r_i)$. Furthermore, the spin-orbit coupling was a key incorporation of the nuclear shell model. The Hamiltonian includes the interaction between the spin and the angular momentum, such that the total momentum of the independent nucleon is $\vec{j} = \vec{l} + \vec{s}$. The spin-orbit coupling defines the splitting of energy levels reproducing beautifully the magic numbers:

$$H_0 = \sum_{i=1}^{A} T(r_i) + V(r_i) + \xi \vec{l_i} \cdot \vec{s_i}, \tag{3}$$

where A is the mass number of the atom, therefore we sum for all nucleons in the nucleus.

The solutions to the Schrödinger equation considering the one-body Hamiltonian are given by Slater determinants, respecting the Pauli exclusion principle. The single-particle states are determined by the n, l, j, m, τ quantum numbers:

$$|\phi_\alpha\rangle = \prod_{i=nlmj\tau} a_i^\dagger |0\rangle , \tag{4}$$

where $a_i^\dagger$ is the creation operator for the i state and $|0\rangle$ is the vacuum state. n is the radial quantum number, l is the orbital quantum number, j is the quantum number associated with the total angular momentum, m is the projection of j, and τ is the isospin quantum number.

Moving away from the concept of nucleon independence, it becomes imperative to acknowledge the presence of residual nucleon-nucleon interactions, captured in W in Eq.(2). Then, in the case of incorporating these nucleon-nucleon interactions, the solutions to the Schrödinger equation are linear combinations of Slater determinants:

$$|\psi\rangle = \sum_\alpha C_\alpha |\phi_\alpha\rangle . \tag{5}$$

Nevertheless, the configuration space grows rapidly with heavier nucleons and an approximation must be made to consider a workable Hilbert space. We differentiate three parts in the Hilbert space: the core, the valence space and the empty space. Firstly, the core which encloses the inactive lowest energy single-particle orbitals usually in closed shells that are not affected by the active nucleons around the Fermi surface. The valence space consists of the single-particle orbitals that are active. Finally, the empty space is composed of orbits that are assumed to be unoccupied due to the large energy gap from the valence space. The single-particle orbital is notated as nl_j, where n, l, j are quantum numbers. In the context of this paper, the valence space encompasses the single-particle orbitals ($1p_{3/2}$, $0f_{5/2}$, $1p_{1/2}$, $0g_{9/2}$). Then the core contains the ($0s_{1/2}$, $0p_{3/2}$, $0p_{1/2}$, $0d_{5/2}$, $1s_{1/2}$, $0d_{3/2}$, $0f_{7/2}$) single-particle orbitals, this is, a ^{56}Ni core.

The Hamiltonian must undergo modifications in order to describe the physics of the nuclear state in the valence space. Ultimately, we operate with effective Hamiltonians, which are subsequently diagonalized within the valence space:

$$H_{eff} |\psi_{eff}\rangle = E |\psi_{eff}\rangle , \tag{6}$$

where $|\psi_{eff}\rangle$ is the wave function describing the state of the system, restricted to the valence space. In this paper, we use the previously calculated effective Hamiltonians: JJ4BB, JUN45, RG545, RGPROLATE [5].

Lanczos Method

In spite of working in the reduced configuration space, direct diagonalization is impractical from a computational point of view due to large dimensions of the matrices. For instance, the effective dimensions of the ^{82}Se and ^{82}Kr nuclei in the defined valence space are $d = 3.6 \cdot 10^5$ and $d = 4.0 \cdot 10^7$, respectively. Hence, the utilization of algorithms becomes very useful to effectively diagonalize these matrices.

In this study, we employ the ANTOINE [6] code for the nuclear shell model, which executes the precise diagonalization of the effective Hamiltonian through the Lanczos method.

III. DOUBLE β DECAY

In the context of the nuclear shell model, we study the $2\nu\beta\beta$ decay from ^{82}Se to ^{82}Kr. The β decay is a nuclear transition where a neutron transforms to a proton while an electron and an antineutrino are produced. In the $2\nu\beta\beta$ decay, this happens twice:

$$(Z, N) \xrightarrow{\beta^-\beta^-} (Z+2, N-2) + 2e^- + 2\overline{\nu}_e, \tag{7}$$

where N and Z are the number of neutrons and protons in the nucleus respectively.

This transition is governed by the Gamow-Teller operator of the form $\hat{O}_{GT} = \sum_i \tau_i^- \sigma_i$, where σ is the Pauli spin operator and τ^- is the isospin operator which transforms neutrons into protons. The sum i is over all the

nucleons in the nucleus. The matrix element of the reaction is as follows.

$$M^{2\nu} = \sum_n \frac{\langle 0_f^+ || \sum_a \tau_a^- \sigma_a || 1_n^+ \rangle \langle 1_n^+ || \sum_b \tau_b^- \sigma_b || 0_i^+ \rangle}{E_n - (E_i - E_f)/2}, \quad (8)$$

where the sum is over all the intermediate states, n. E_n is the energy of the n intermediate state, and E_i and E_f are the initial state and final state energies, respectively, taken from experimental data.

The calculation of this matrix element comprises the following sequential steps. Initially, we determine the wave function of the initial state $|0_i^+\rangle$ of ^{82}Se. Subsequently, we apply the Gamow-Teller operator to the initial state, resulting in the generation of intermediate $|1_n^+\rangle$ states of ^{82}Br:

$$\hat{O}_{GT} \, |^{82}\mathrm{Se}\rangle = |^{82}\mathrm{Br}^*\rangle = \sum_n a_n \, |1_n^+\rangle \, . \quad (9)$$

The number of intermediate states considered, $|1_n^+\rangle$, is not infinite. We have verified that the inclusion of 20 intermediate states results in complete convergence of the $M^{2\nu}$ values in Eq.(8).

Simultaneously, we determine the wave function of the final state $|0_f^+\rangle$ of ^{82}Kr. Then, we apply the Gamow-Teller operator to the final state $|0_f^+\rangle$ of ^{82}Kr.

$$\hat{O}_{GT} \, |^{82}\mathrm{Kr}\rangle = |^{82}\mathrm{Br'}^*\rangle \, . \quad (10)$$

Finally, we compute the overlap between the obtained state and the previously calculated $|1_n^+\rangle$ states of ^{82}Br.

The associated half-life is:

$$(T_{1/2}^{2\nu})^{-1} = G^{2\nu} g_A^4 (M^{2\nu} m_e c^2)^2, \quad (11)$$

where $G^{2\nu}(0_{gs}^+) = 1596 \cdot 10^{-21}\ y^{-1}$, $G^{2\nu}(0_2^+) = 4.8 \cdot 10^{-21}\ y^{-1}$ are the phase-space factors [7], $g_A = 1.27$ is the axial nucleon coupling and m_e is the electron mass.

Nevertheless, these shell-model matrix elements are known to underestimate half-life values. In order to match the experimental data a 'quenching' factor is introduced. We work with a quenching factor previously calculated, $q_\beta = 0.6$, as reference [8]. Alternatively, we obtain a quenching factor from comparing our calculated matrix elements with the experimental ones for the well-known half-life for the ground state to ground state $2\nu\beta\beta$ decay [9].

IV. RESULTS AND DISCUSSION

First, we assess the validity of the employed interactions. Fig. 1 compares the calculated low-lying spectra to the experimental one of ^{82}Se. We observe that the ground state is well reproduced across all the interactions. Furthermore, we see that JJ4BB, JUN45 and RG545 reproduce similarly well the first excited state 2^+. These three interactions demonstrate a reasonably close agreement

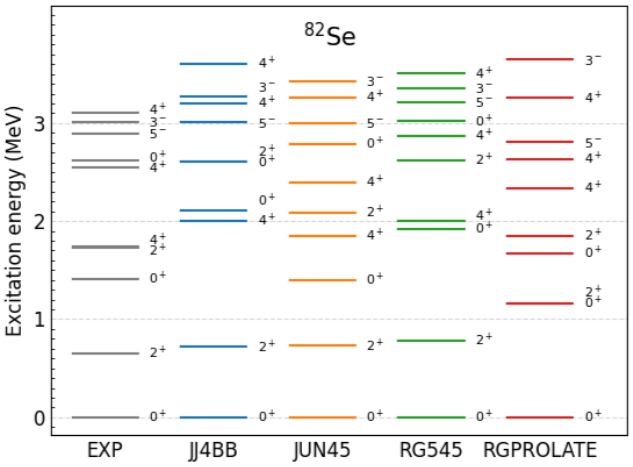

FIG. 1: ^{82}Se spectra for the 10 lowest-energy states calculated using the four shell model interactions, compared to experimental data [10]. Each level is labeled by the total angular momentum and parity, J^P.

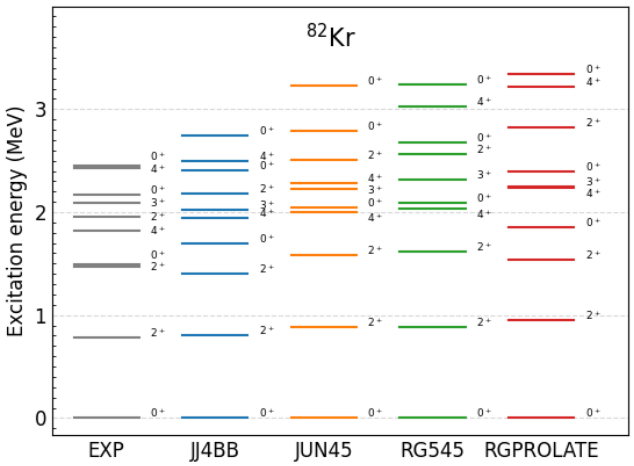

FIG. 2: Same as Fig. 1 but for the 10 lowest-lying states of ^{82}Kr.

with the experimentally observed states. It is noticeable that JUN45, while not showing the grouping structure seen in the experimental data, yields the least errors in individual state reproductions. On the contrary, JJ4BB, still aligning reasonably well with the experimental data, does exhibit the measured grouping behavior of excited states. Lastly, RGPROLATE seems to be the least descriptive of the nuclear structure, as neither the grouping nor the energy of the levels agrees well with data.

Concerning the spectra of ^{82}Kr, Fig. 2, across all interactions both the ground state and the first excited state are well reproduced. In the interest of our study, we focus on the first 0_2^+ excited state. Notably, the interactions JJ4BB and RGPROLATE describe better the energy of this particular excited state. On the other

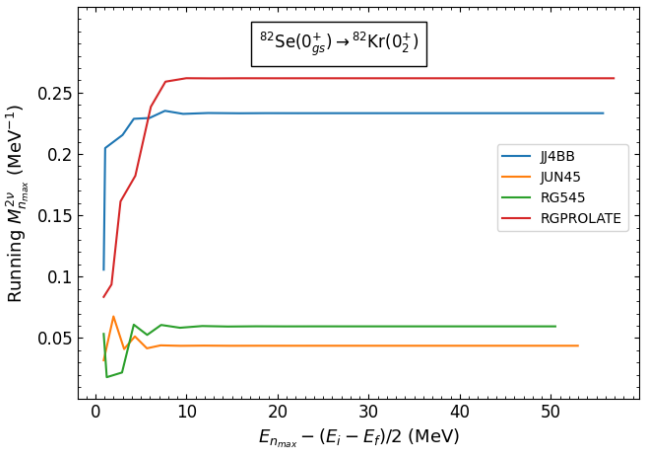

FIG. 3: Running $M^{2\nu}(0^+_2)$ matrix element for the decay of 0^+_{gs} of ^{82}Se to the first excited state 0^+_2 of ^{82}Kr. Plotted against the energy denominator corresponding to the excited state n in Eq.(8) .

hand, the JUN45 and RG545 interactions estimate a relatively higher energy for this excited state than experiment. Fig. 2 shows that the JJ4BB interaction agrees better with experimental data compared to other interactions.

We undertake a more in-depth analysis, focusing now on the nuclear wave functions characterizing the states, in the context of shell occupation. The most relevant eigenstates for ^{82}Se, $|0^+_i\rangle$, are, for the different interactions:

$$\begin{aligned}
&\text{JJ4BB:} && |0^+_{gs}\rangle = 0.60\,|8\,2\,6\,4\,0\,0\,4\,2\rangle + ...\\
&\text{JUN45:} && |0^+_{gs}\rangle = 0.62\,|8\,2\,6\,4\,0\,0\,4\,2\rangle + ...\\
&\text{RG545:} && |0^+_{gs}\rangle = 0.61\,|8\,2\,6\,4\,0\,0\,4\,2\rangle + ...\\
&\text{RGPROLATE:} && |0^+_{gs}\rangle = 0.44\,|10\,0\,6\,4\,0\,0\,6\,0\rangle\\
&&& \quad + 0.32\,|10\,0\,6\,4\,0\,0\,4\,2\rangle + ...,
\end{aligned}$$

where we have only considered contribution with $|C_\alpha|^2 \geq 0.1$ in Eq.(5). The ket in the right side of the equation above represents $|n_{g_{9/2}} n_{p_{1/2}} n_{f_{5/2}} n_{p_{3/2}} p_{g_{9/2}} p_{p_{1/2}} p_{f_{5/2}} p_{p_{3/2}}\rangle$, with n_i, p_i the occupation number of orbitals for neutrons and protons respectively.

The ground states of ^{82}Se are similar for the JJ4BB, JUN45, and RG545 interactions, with a common state representing the most substantial contribution to the wave function. In contrast, the RGPROLATE interaction manifests a more fragmented wave function, having no dominant configuration.

The same analysis for the 0^+_2 state in ^{82}Kr shows that JUN45 and RG545 predict a dominant configuration while JJ4BB and RGPROLATE encompass a broader fragmentation of Slater determinants contributing to the characterization of the 0^+_2 state.

Next, we study the $2\nu\beta\beta$ matrix elements. We define the running matrix element for the nth state as the matrix element obtained considering a number of intermediate states equal to n, Eq.(12):

$$M^{2\nu}_{n_{\max}} = \sum_{n}^{n_{\max}} M^{2\nu}_{n}, \tag{12}$$

with $M^{2\nu} = \sum_n M^{2\nu}_n$ in Eq.(8). Fig. 3 shows this running matrix element as a function of the energy denominator associated to the intermediate state $|1^+_n\rangle$ of ^{82}Br.

The running matrix element converges for a number of intermediate states. For the decay involving the first 0^+_2 excited state decay this convergence occurs at energies $E \sim 12$ MeV. Additionally, the most significant contributions to the running matrix element originate from the lowest-energy excited states. Fig. 3 reveals that the most prominent contribution originates from just the first excited state in case of the JJ4BB interaction.

Fig. 3 shows the running $2\nu\beta\beta$ matrix element to the decay of ^{82}Se to the 0^+_2 state of ^{82}Kr, as a function of the energy denominator in Eq.(8). Fig. 3 shows two distinct groupings of behaviour. Firstly, in the case of JJ4BB and RGPROLATE, there are no cancellations between the contributions of the different terms, with all intermediate states contributing with the same sign. Conversely, with JUN45 and RG545, the contributions of the different intermediate states are of different sign, resulting in cancellations, particularly notable in the lowest excited states. Therefore, JUN45 and RG545, show a smaller matrix element, consequently leading to a longer half-life. The two latter interactions showed worse agreement with experimental data when describing the 0^+_2 final state.

Theoretical calculations of matrix elements and half-lives in this context, must be typically corrected by a 'quenching' factor to match the experimental observations. The quenching factor involved in the correction of these matrix elements, is adopted from literature as reference $q_\beta = 0.6$, determined from β decays comparing theory to experiment [8]. We alternatively compute the quenching factor so that our calculations of the $2\nu\beta\beta$ decay to the ground state match the experimental data for the well-established half-life $T^{2\nu}_{1/2}(^{82}\text{Se}, 0^+_{gs} \to 0^+_{gs}) = 8.69 \cdot 10^{19}$ yr [2]. Thus, we derive our results using a quenching interval, $(q_\beta, q_{2\nu})$.

Table I summarizes the quenching interval used in the calculations of half-lives for the different interactions. We observe that only for RGPROLATE the two values of q

TABLE I: Quenching factor values used for the calculation of $2\nu\beta\beta$-decay half-lives. We present q_β, the reference value, and the calculated quenching factor for each interaction, $q_{2\nu}$.

	q_β	$q_{2\nu}$
JJ4BB	0.6	0.56
JUN45	0.6	0.55
RG545	0.6	0.54
RGPROLATE	0.6	0.44

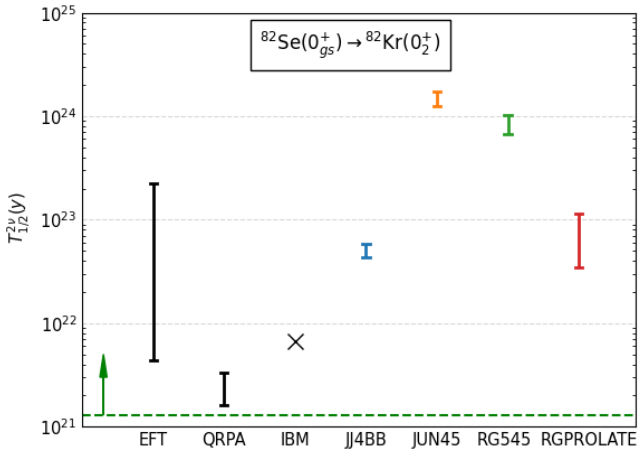

FIG. 4: ^{82}Se $2\nu\beta\beta$-decay half-life to the first 0^+_2 excited state of ^{82}Kr obtained with the different interactions. The results are compared with previously calculated values (in black) with different methods: EFT [11], QRPA [12], IBM [13]. The dashed line and arrow indicates the experimental limit for this transition [4].

are significantly different. This results in a larger range of half-life predictions for this interaction, as shown in Figure 4. Figure 4 summarizes the results of our calculation of the half-lives compared to previously calculated half-life values as well as the experimental limit. We can see all of our interactions are consistent with the experimental limit $T^{2\nu}_{1/2}(^{82}\text{Se}, 0^+_{gs} \to 0^+_2) > 1.3 \cdot 10^{21}$ yr [4]. One can also notice that we have predicted longer half-lives than the ones obtained through other methods. It is noticeable that the JJ4BB and RGPROLATE interactions, which seemed to describe better the final state, give results more similar to the values from the literature. We see between these predictions orders of magnitude of difference. The discrepancies in the prediction make testing these half-life values experimentally a good way to validate the many-body methods used for the calculation of matrix elements.

V. CONCLUSIONS

In summary, our investigation into $2\nu\beta\beta$ decay has encompassed various methodologies applicable to the study of $0\nu\beta\beta$ decay. Specifically, we focused on computing the half-life for the transition of ^{82}Se to the first 0^+_2 excited state of ^{82}Kr. This analysis was conducted within the framework of the nuclear shell model, for four different interactions. We compared the spectra predicted by the interactions to the experimental data, for both nuclei, ^{82}Se and ^{82}Kr. Furthermore, we computed and analyzed the running matrix element for these interactions.

Finally, we have determined half-live for four different interactions. The range of the predicted half-lives for the different interactions in our study is $T^{2\nu}_{1/2}(^{82}\text{Se}, 0^+_{gs} \to 0^+_2) = (3.5-170)\cdot 10^{22}$ yr. If we just keep the results from our shell-model interactions that best describe the 0^+_2 state in ^{82}Kr, the predicted half-life is $T^{2\nu}_{1/2}(^{82}\text{Se}, 0^+_{gs} \to 0^+_2) = (3.5 - 11.4) \cdot 10^{22}$ yr. Despite these results being within experimental limits, we predicted longer half-lives than previous studies with different methods. We look forward to these half-life values being tested in upcoming experiments.

Acknowledgments

I would like to show my gratitude to my advisor Javier Menéndez for his support, guidance, knowledge and time. I would also like to thank my family and friends, for listening all these years to my lectures, complaints, passions and ideas.

[1] M. Agostini, G. Benato, J. A. Detwiler, J. Menéndez, F. Vissani. Rev. Mod. Phys. 95: 025002 (2023).
[2] O. Azzolini et al. Phys. Rev. Lett. 131: 222501 (2023).
[3] A. Poves, E. Caurier, A. P. Zuker. Phys. Rev. C 53: R2602(R) (1996).
[4] NEMO-3 collaboration. Nuc. Phys. A 996: 121701 (2020).
[5] A. Poves, F. Nowacki. "The nuclear shell model". Springer (2001).
[6] E. Caurier, F. Nowacki. Acta Phys. Pol. B 30: 705 (1999).
[7] S. Stoica, M. Mirea. Front. Phys. 7: 12 (2019).
[8] E. Caurier, F. Nowacki, A. Poves. Phys. Lett. B 711: 1, 62-64 (2012).
[9] A. Barabash. Universe. 6(10): 159 (2020).
[10] Brookhaven National Laboratory. National Nuclear Data Center. https://www.nndc.bnl.gov (2023).
[11] E. A. Coello Pérez, J. Menéndez, A. Schwenk. Phys. Rev. C 98: 045501 (2018).
[12] J. Toivanen, J. Suhonen. Phys. Rev. C 55: 2314 (1997).
[13] J. Barea, J. Kotila and F. Iachello. Phys. Rev. C 91: 034304 (2015).